

A Dual-Responsive Ratiometric Fluorescent Probe for the Detection of Hypochlorite and Hydrazine in Environmental Samples, Live Cells, and Plant Tissues

Dipanjana Banik^a, Shilpita Banerjee^a, Satyajit Halder^b, Rajdeep Ganguly^c, Anirban Karak^a,
Pintu Ghosh^a, Kuladip Jana^b, Ajit Kumar Mahapatra^{a*}

^aMolecular Sensor and Supramolecular Chemistry Laboratory, Department of Chemistry,
Indian Institute of Engineering Science and Technology, Shibpur, Howrah-711103, West
Bengal, India.

^bDivision of Molecular Medicine, Bose Institute, P 1/12, CIT Scheme VIIM, Kolkata 700054,
India.

^cCentre for Healthcare Science and Technology, Indian Institute of Engineering Science and
Technology, Shibpur, Howrah-711103, West Bengal, India.

*Author to whom correspondence should be addressed; electronic mail:

akmahapatra@chem.iiests.ac.in; Tel.: +91 – 9434508013

Contents

Description	Page
1. Experimental section.....	S3-S6
2. Table S1 Crystal Data and Structure Refinement Parameters of the probe PIID	S7
3. Plot of absorbance ratio change of PIID against different concentrations of ClO^-	S8
4. Plot of absorbance ratio change of PIID against different concentrations of N_2H_4	S8
5. Emission spectra of PIB	S9
6. Plot of fluorescence change of PIID against different concentrations of ClO^-	S9
7. Plot of fluorescence change of PIID against different concentrations of Hydrazine.....	S10
8. Fluorescence linear fit graph to determine the detection limit for hydrazine.....	S10
9. Calculation of fluorescence quantum yield of PIID in the presence and absence of ClO^- and N_2H_4	S10-S11
10. Selectivity study.....	S11
11. Time-dependent emission ratios change with time of the reaction of PIID with N_2H_4	S11
12. Determination of rate constant (k_{obs}) of the reaction of PIID with N_2H_4	S12
13. Investigation of the reaction mechanism by using HRMS spectra.....	S12-S13
14. Table S2 The main vertical orbital transition of the Probe PIID and the resulting compounds PIB and PIBH calculated by TD-DFT method.....	S13
15. MTT assay.....	S14
16. Table S3 Environmental water sample study for ClO^- detection	S14
17. Table S4 Environmental water sample study for N_2H_4 detection	S14
18. Fluorescence spectra of probe for commercial sample.....	S15
19. ^1H -NMR and ^{13}C -NMR spectrum of PIB and PIID	S15-S17
20. IR spectra of probe PIID	S17
21. ESI-MS Spectra of PIB and PIID	S18
22. Comparison Table S5 between reported ClO^- probes with our probe PIID	S19
23. Comparison Table S5 between reported N_2H_4 probes with	

our probe PIID	S20
24. References	S21

1. Experimental section

Materials and instrumentation

The chemicals of Sigma-Aldrich company were used directly for synthesis purposes. Commercially supplied analytical grade solvents were used for all experiments. 100-200 mesh Silica gel (Spectrochem Pvt. Ltd. Mumbai, India) was used in column chromatography to purify products, and Merck silica gel 60 F₂₅₄ plates were used for thin layer chromatography (TLC). UV-vis spectra were done by using a Shimadzu UV-1800 UV-vis spectrophotometer. A fluorescence spectrophotometer (Model 1057, Fluorolog, Horiba Scientific, USA) was used for recording Fluorescence spectra. ¹H and ¹³C NMR spectra were performed using Bruker Avance 400 MHz instrument where DMSO-d₆ was used as solvent and TMS as an internal standard. Mass spectra were carried out using a Waters Q-TOF YA 263 mass spectrometer.

The general method of UV-vis and fluorescence titration

Spectral measurements were done by preparing a stock solution of the probe **PIID** in a THF/H₂O solution (3:7 and 4:6 v/v; 10 mM PBS buffer, pH 7.4) by filling a quartz optical cell having a 1cm optical path length was filled with 2 ml probe solution (10⁻⁵M) and both the titration experiments were done by continuous addition of a 10 μM analyte stock solution (10⁻⁴M) to this probe solution by using a micropipette.

Cell line study

To conduct our investigation, we acquired the NKE human kidney epithelial cell line, MDA-MB 231 human breast cancer cell line, and RAW 264.7 macrophage cell line from the National Center for Cell Science (NCCS) in Pune, India. The cells were cultivated in T25 flasks using Dulbecco's Modified Eagle Medium (DMEM), meticulously supplemented with 10% fetal bovine serum (FBS), 1 mM sodium pyruvate, 2 mM L-glutamine, non-essential amino acids, and a comprehensive antibiotic mix comprising 100 U/mL penicillin, 100 mg/L streptomycin, and 50 mg/L gentamycin. To maintain cell viability and promote optimal growth conditions, the cultures were housed in a humidified incubator set at 37 °C with 5% CO₂.

Cytotoxicity assay

The cytotoxicity of the **PIID** probe was assessed via the MTT cell proliferation assay¹ on MDA-MB-231 breast cancer cells, NKE normal kidney epithelial cells, and RAW 264.7 macrophage cells. Cells were seeded in 96-well plates at a density of 1 × 10⁴ cells per well and incubated for 24 hours to allow adherence. Subsequently, cells were treated with a range of **PIID** probe concentrations (0 μM, 10 μM,

20 μ M, 30 μ M, 40 μ M, 80 μ M, and 100 μ M) for a 24-hour exposure period. After treatment, the culture medium was removed, and cells were rinsed with 1x PBS. MTT solution at 0.5 mg/mL was added to each well, and cells were incubated for 4 hours. After incubation, cells were rinsed again with PBS, and the resulting formazan crystals were solubilized in DMSO. Absorbance was measured at 570 nm using a microplate reader. Cell viability was calculated as a percentage relative to untreated control cells.

Exogenous and endogenous hypochlorite imaging

Fluorescence imaging was conducted on MDA-MB-231 cells to investigate the fluorescence properties of the **PIID** probe in response to hypochlorite (5 μ M and 10 μ M). Cells were cultured on coverslips for 24 hours at 37°C in a humidified atmosphere containing 5% CO₂. The cells were then pretreated with hypochlorite at concentrations of 5 μ M and 10 μ M for 20 minutes. After washing with PBS, the cells were treated with 10 μ M of the **PIID** probe and incubated for 20 minutes. A final PBS wash was performed to remove any unbound **PIID**, and the cells were mounted on glass slides for imaging using an Olympus fluorescence microscope.

To further evaluate the in vivo hypochlorite sensing ability of **PIID**, RAW 264.7 macrophages were similarly cultured on coverslips for 24 hours at 37°C in a humidified environment with 5% CO₂. The cells were pretreated with lipopolysaccharide (LPS) at 1 μ g/mL concentrations and 2 μ g/mL for 3 hours. After PBS washing, they were treated with 10 μ M of the **PIID** probe and incubated for 20 minutes. Following another PBS wash, the cells were mounted on glass slides and visualized using an Olympus fluorescence microscope.

Since NAC (N-acetyl cysteine) is known to reduce intracellular hypochlorite levels, in a separate experimental setup, RAW 264.7 cells pretreated with LPS (2 μ g/mL) + N-acetyl cysteine (NAC) were exposed to 10 μ M of the **PIID** to confirm the specificity of the **PIID** probe's fluorescence response to hypochlorite.

Synthesis of the probe

Synthesis and characterization of 4-(1H-phenanthro[9,10-d] imidazol-2-yl) benzaldehyde (PIB):

10 ml Acetic acid was added to a mixture of 9,10-phenanthroquinone (500 mg, 2.40 mmol) and terephthalaldehyde (966 mg, 7.20 mmol) followed by the addition of ammonium acetate (3.70 g, 48 mmol) and stirred for 2hr at 100°C. Then, the reaction mixture was cooled to room temperature, and the precipitate was filtered through filter paper. After that, it was washed with acetate acid, dilute sodium hydrogen carbonate solution, and water successively. Finally, after vacuum drying, the precipitate was purified by column chromatography on silica gel (eluent: acetone) to afford yellow crystalline solid **PIB** (588 mg, yield~75.8%)

¹H NMR (400 MHz, DMSO): δ 13.73 (s, 1H), 10.10 (s, 1H), 8.87 (dd, J = 14.8, 8.3 Hz, 2H), 8.60 (dd, J = 15.1, 7.5 Hz, 2H), 8.53 (d, J = 8.3 Hz, 2H), 8.14 (d, J = 8.4 Hz, 2H), 7.77 (dt, J = 14.9, 7.3 Hz, 2H), 7.66 (dt, J = 8.4, 4.3 Hz, 2H).

¹³C NMR (101 MHz, DMSO): δ 193.06 (s), 148.16 (s), 137.89 (s), 136.52 (s), 135.90 (s), 130.70 (s), 128.83 (s), 128.54 (s), 128.21 (s), 127.82 (s), 127.70 (s), 127.30 (s), 126.92 (s), 126.32 (s), 125.99 (s), 124.66 (s), 124.30 (s), 122.73 (s), 122.69 (s), 122.41 (s).

HRMS (ESI): *m/z* (%): 323.1175 [**PIB** + H]⁺ (Calc. for C₂₂H₁₅N₂O⁺: 323.1178)

Synthesis and characterization of 2-(4-(1H-phenanthro[9,10-d] imidazol-2-yl) benzyldiene)-1H-indene-1,3(2H)-dione (PIID):

7 ml of anhydrous ethanol was added to a mixture of **PIB** (300 mg, 0.93 mmol) and 1,3-indanedione (164 mg, 1.12 mmol) in a two-neck round bottom flask under a nitrogen atmosphere and blended for 15 minutes. Then, two drops of piperidine were added and refluxed overnight. Afterward, the reaction mixture was cooled to room temperature, filtered, and washed with cold ethanol. Finally, the precipitate was subjected to column chromatography using 1% ethyl acetate in DCM to obtain a floppy red solid of **PIID** as the pure product (185 mg, yield~ 44.15%).

IR (cm⁻¹): 3330 (ν, N-H), 1716 (ν, C=O), 1667 (ν, C=O), 1578 (ν, C=N).

¹H NMR (400 MHz, DMSO): δ 13.70 (s, 1H), 8.87 (dd, *J* = 14.5, 8.3 Hz, 2H), 8.75 (d, *J* = 8.5 Hz, 2H), 8.60 (dd, *J* = 18.7, 7.1 Hz, 2H), 8.48 (d, *J* = 8.5 Hz, 2H), 8.07 – 7.94 (m, 4H), 7.91 (s, 1H), 7.83 – 7.72 (m, 2H), 7.67 (q, *J* = 7.2 Hz, 2H).

¹³C NMR (101 MHz, DMSO): δ 189.17 (s), 189.15 (s), 148.39 (s), 144.88 (s), 142.50 (s), 140.01 (s), 138.34 (s), 138.04 (s), 136.54 (s), 136.50 (s), 136.36 (s), 136.34 (s), 135.17 (s), 135.10 (s), 134.50 (s), 133.68 (s), 133.67 (s), 133.28 (s), 129.88 (s), 129.83 (s), 128.56 (s), 127.83 (s), 127.77 (s), 126.44 (s), 123.67 (s), 123.56 (s), 122.68 (s).

HRMS (ESI): *m/z* (%): 451.1439 [**PIID** + H]⁺. (Calc. for C₃₁H₁₉N₂O₂⁺: 451.1441)

Sources of RONS:

H₂O₂: It was sourced commercially. The concentration was estimated using KMnO₄ titration and then used directly.

O₂^{•-}: It was generated by adding KO₂ to dry DMSO and vigorously stirring for 10 minutes.

¹O₂: It was produced in situ by adding a hypochlorite stock solution (50 mM in H₂O) to a solution with a large excess of H₂O₂.

NO: It was obtained from sodium nitroprusside solution, which is commercially available.

ClO⁻: It was obtained from commercially available sodium hypochlorite.

ONOO⁻: Peroxynitrite was prepared by mixing sodium nitrite (1.2 M), hydrogen peroxide (1.4 M), and HCl (1.2 M) in an ice bath, followed by the addition of NaOH solution (3 M). Excess hydrogen peroxide was removed by passing the solution through a manganese dioxide column, and the required concentration was then adjusted accordingly.

$\cdot\text{OH}$: It was generated using the Fenton process. Twenty milligrams of FeCl_2 were added to 10 equivalents of H_2O_2 , assuming the $\cdot\text{OH}$ concentration to be equal to that of Fe^{2+} . The solution was then diluted to the required concentration.

Crystal structure of the probe **PIID**

The structure of the probe **PIID** was characterized by X-ray diffraction analysis of its single crystal (Fig.S1), which was grown by slow evaporation in the solvent mixture of THF/Hexane at room temperature. The CCDC entry no. is **2355056** for our crystal structure obtained from the Cambridge Crystallographic Data Centre. **PIID** was crystallized in the Monoclinic crystal system, belonging to the P 2₁/c space group. we got the hydrated form of the probe **PIID** as its single crystal contains three H_2O molecules. In crystal packing (Fig.S2), strong H- H- bonding interaction was found between $\text{N2-H7}\cdots\text{O4}$, $\text{N1}\cdots\text{H5A}$, and $\text{O5}\cdots\text{H4A}$. Crystallographic parameter and structure refinement details are presented in Table S1.

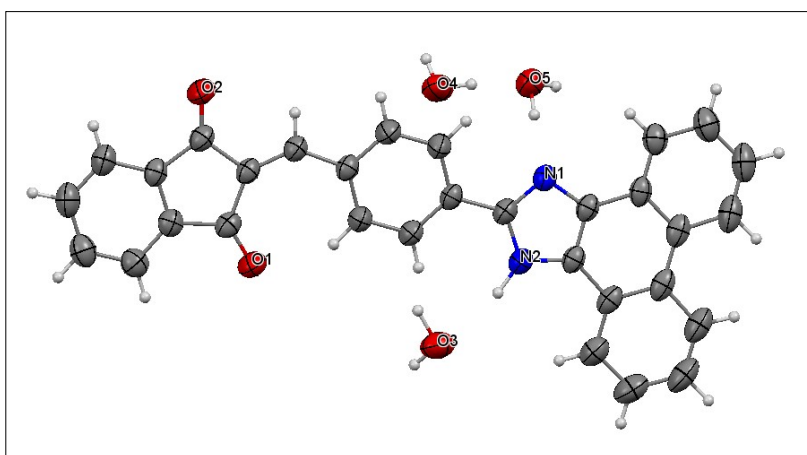


Fig. S1 ORTEP diagram of **PIID** with ellipsoid at 50% probability.

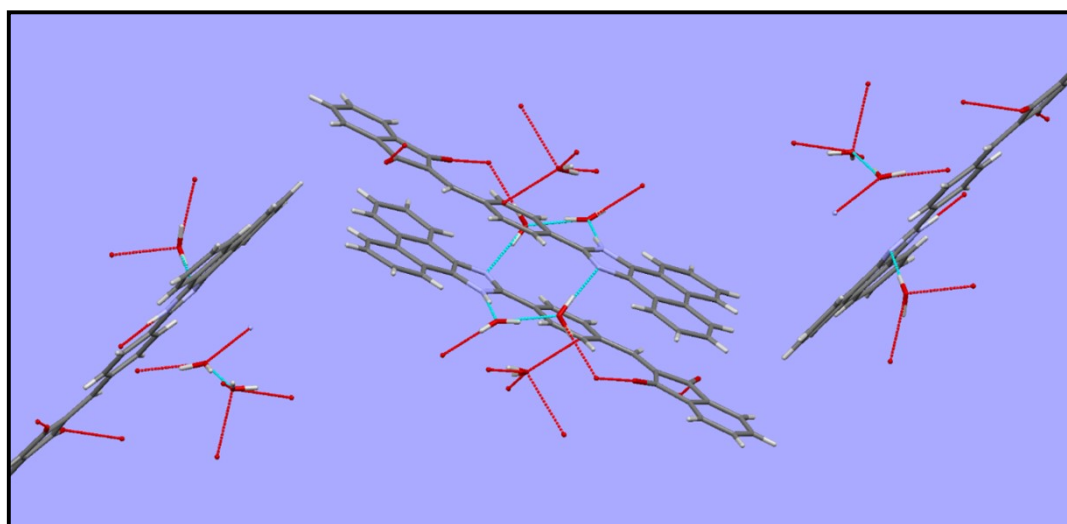


Fig. S2 H- bonding interaction was found between $\text{N2-H7}\cdots\text{O4}$, $\text{N1}\cdots\text{H5A}$, and $\text{O5}\cdots\text{H4A}$ in the crystal packing of the probe **PIID**.

2. Table S1 Crystal Data and Structure Refinement Parameters of the probe PIID

Empirical formula	C ₃₁ H ₁₈ N ₂ O ₂ , 3(H ₂ O)
Formula Weight	504.52
Temperature (K)	250
Wavelength (Å)	0.71073
Crystal system	Monoclinic
space group	P 21/c
a, b, c (Å)	8.5019(6), 31.998(2), 9.5689(6)
α, β, γ (°)	90, 109.195(2), 90
Volume (Å ³)	2458.4(3)
Z / Density (calc.) (Mg/m ³)	4/ 1.363
Absorption coefficient (mm ⁻¹)	0.093
F (000)	1056.0
θ range for data collection	2.537 to 27.207
Absorption correction	Multi-scan
Max. and min. transmission	0.953 and 0.944
Refinement method	Full-matrix least-squares on F ²
Data/parameters	5448/ 371
Goodness-of-fit on F ²	0.950
Final R indices [I > 2σ(I)]	R ₁ = 0.0511, wR ₂ = 0.1351
R indices (all data)	R ₁ = 0.1037, wR ₂ = 0.1926
Largest diff. peak and hole (e.Å ⁻³)	0.165 and -0.194

$R_1 = \sum ||F_o| - |F_c|| / \sum |F_o|$, $wR_2 = [\sum \{(F_o^2 - F_c^2)^2\} / \sum \{w(F_o^2)^2\}]^{1/2} w = 1 / \{\sigma^2(F_o^2) + (aP)^2 + bP\}$, $P = (F_o^2 + 2F_c^2) / 3$, where, $a = 0.1000$ and $b = 1.0379$.

3. Plot of absorbance ratio change of PIID against different concentrations of ClO^-

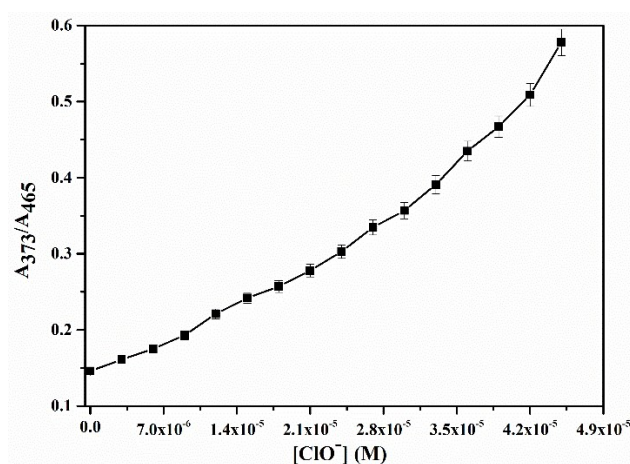


Fig. S3 Change of the absorbance ratio (A_{373}/A_{465}) of the probe PIID upon the addition of different concentrations of ClO^- . Error bars indicate standard deviations of three independent measurements.

4. Plot of absorbance ratio change of PIID against different concentrations of N_2H_4

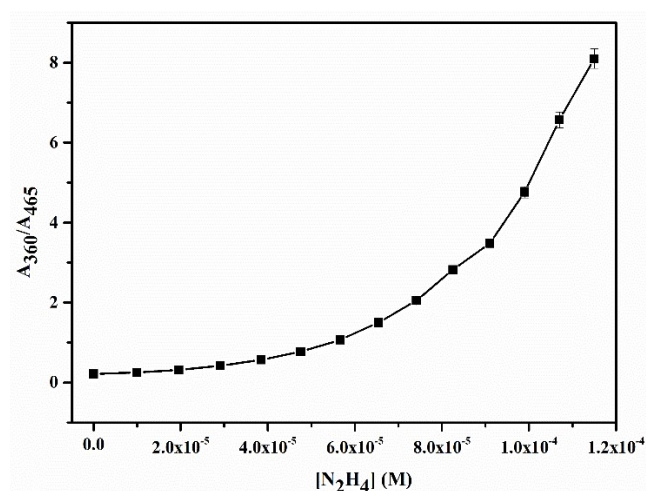


Fig. S4 Change of the absorbance ratio (A_{360}/A_{465}) of the probe PIID upon addition of different concentrations of N_2H_4 . Error bars indicate standard deviations of three independent measurements.

5. Emission spectra of PIB

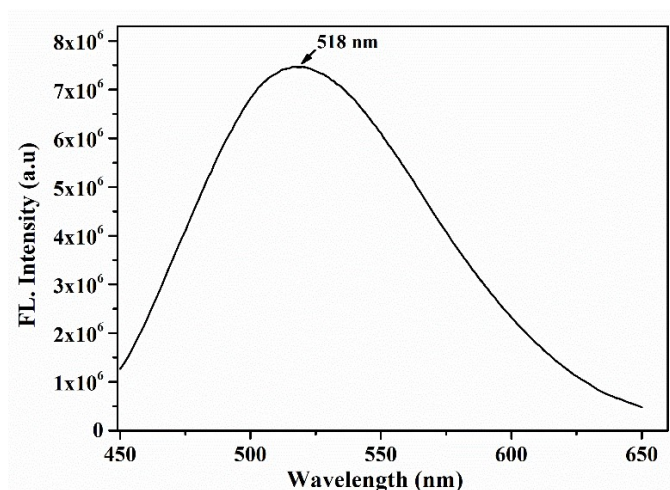


Fig. S5. Emission spectra of **PIB** (1×10^{-5} M) in THF/H₂O solution (3:7, v/v; 10 mM PBS buffer, pH 7.4) ($\lambda_{\text{ex}} = 440$ nm, $\lambda_{\text{em}} = 518$ nm).

6. Plot of fluorescence change of PIID against different concentrations of ClO⁻

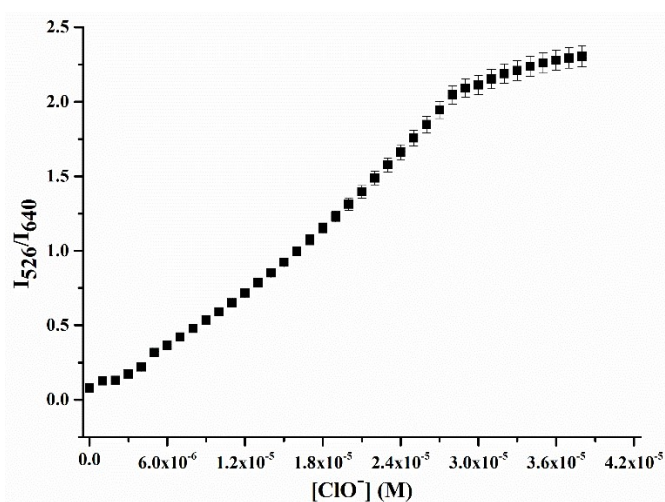


Fig. S6 The plot of fluorescence intensity vs concentration of ClO⁻. Error bars indicate standard deviations of three independent measurements.

7. Plot of fluorescence change of PIID against different concentrations of hydrazine

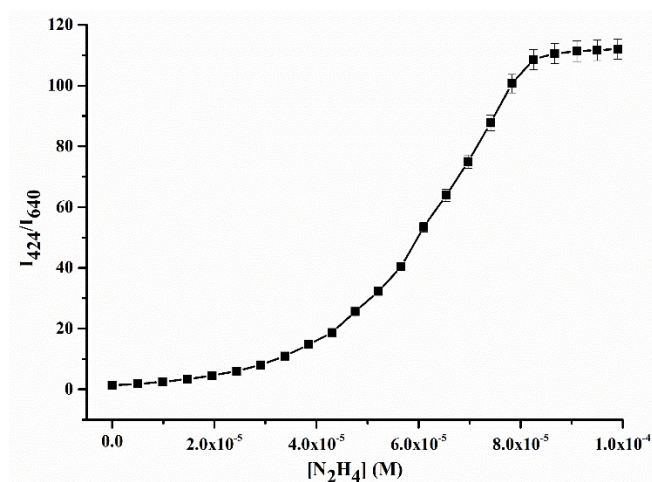


Fig. S7 The plot of fluorescence intensity vs concentration of hydrazine. Error bars indicate standard deviations of three independent measurements.

8. Fluorescence linear fit graph to determine the detection limit for hydrazine

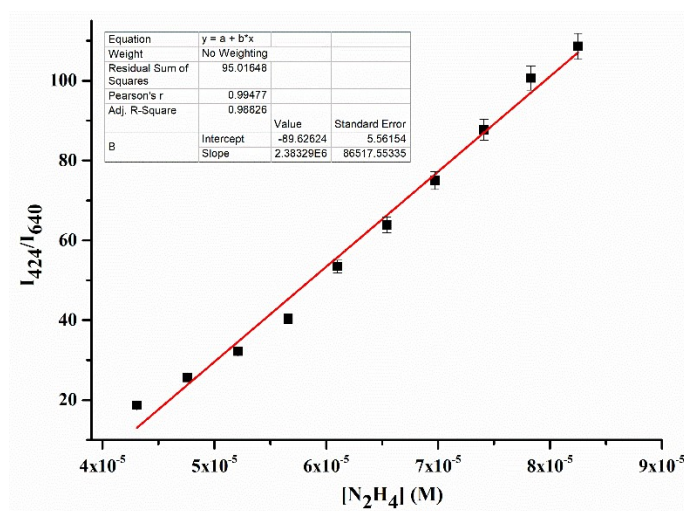


Fig. S8 The fluorescence linear fit graph ($R^2 = 0.98826$) within the concentration range 43 - 83 μM of N_2H_4 to determine the detection limit from the slope (K) obtained is 2.38×10^6 . Error bars indicate standard deviations of three independent measurements.

9. Calculation of fluorescence quantum yield of PIID in the presence and absence of ClO^- and N_2H_4

Here, the fluorescence quantum yield Φ was calculated by using the following equation:

$$\Phi_x = \Phi_s (F_x / F_s) (A_s / A_x) (\eta_x^2 / \eta_s^2)$$

Where, X and S indicate the unknown and standard solution respectively, Φ = quantum yield, F = Area under the emission curve, A = Absorbance at the excitation wavelength, η = Refractive index of solvent.

Here Φ measurements were performed using Rhodamine B in ethanol as standard [$\Phi = 0.70$]. $\eta_s = 1.361$ (for ethanol); $\eta_x = 1.407$ (for THF)

In the absence of ClO^- , the calculated quantum yield (Φ_x) for probe **PIID** = 0.0897. where, $\Phi_s = 0.70$, $F_x = 1.58 \times 10^9$, $F_s = 2.37 \times 10^8$, $A_s = 0.0041$, $A_x = 0.228$.

In the presence of ClO^- , the calculated quantum yield (Φ_x) = 0.1150. Where, $\Phi_s = 0.70$, $F_x = 2.02 \times 10^9$, $F_s = 2.37 \times 10^8$, $A_s = 0.0041$, $A_x = 0.228$.

In the presence of N_2H_4 , the quantum yield was calculated by using quinine sulfate in 0.5M H_2SO_4 as standard [$\Phi = 0.546$]. $\eta_s = 1.346$ (for 0.5M H_2SO_4); $\eta_x = 1.407$ (for THF). The calculated quantum yield (Φ_x) = 0.10. Where, $\Phi_s = 0.546$, $F_x = 6.69 \times 10^8$, $F_s = 1.2 \times 10^9$, $A_s = 0.074$, $A_x = 0.247$.

10. Selectivity Study

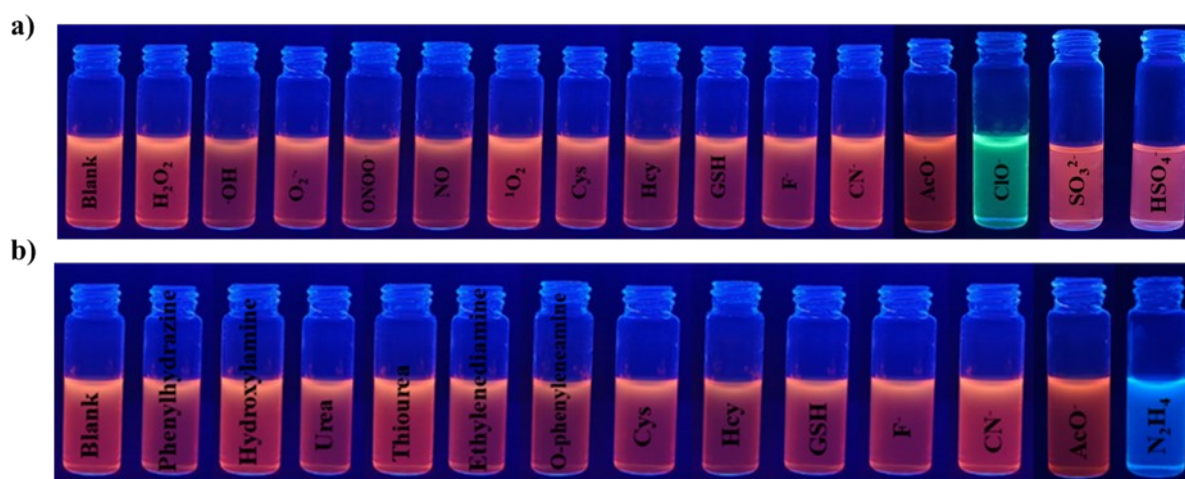


Fig. S9 Fluorescence color change of the probe **PIID** a) in THF/ H_2O solution (3:7, v/v; 10 mM PBS buffer, pH 7.4) b) in THF/ H_2O solution (4:6, v/v; 10 mM PBS buffer, pH 7.4) upon the addition of various analytes under a UV lamp.

11. Time-dependent emission ratios change with time of the reaction of **PIID** with N_2H_4

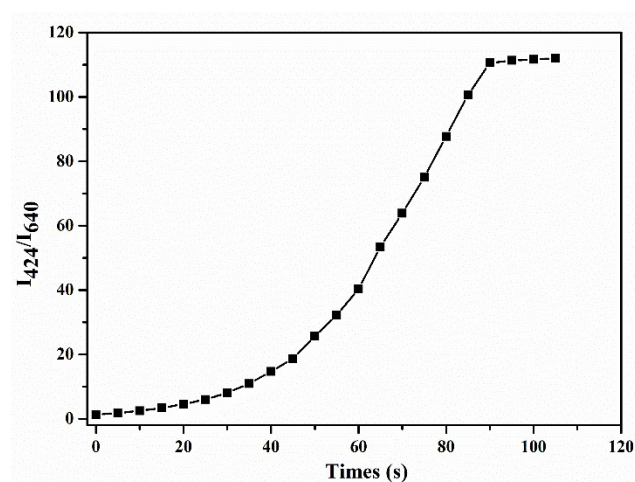


Fig. S10 Time-dependent emission ratios of **PIID** in THF/ H_2O solution (4:6, v/v; 10 mM PBS buffer, pH 7.4) in the presence of 99 μM of N_2H_4 respectively ($\lambda_{\text{ex}} = 420 \text{ nm}$ & 340 nm).

12. Determination of rate constant (k_{obs}) of the reaction of PIID with N_2H_4

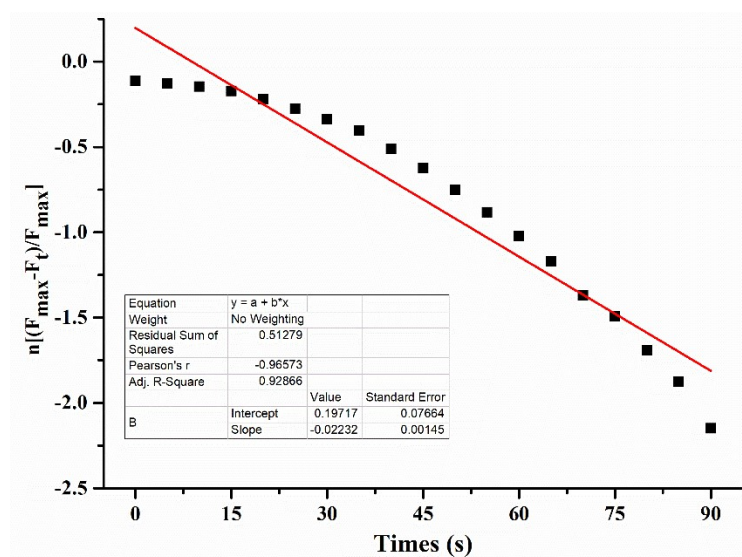


Fig. S11 The kinetic plots to determine the pseudo-first-order rate constant (k_{obs}) of the reaction of **PIID** with N_2H_4 (99 μM) at room temperature in THF/ H_2O solution (4:6, v/v; 10 mM PBS buffer, pH 7.4).

13. Investigation of the reaction mechanism by using HRMS spectra

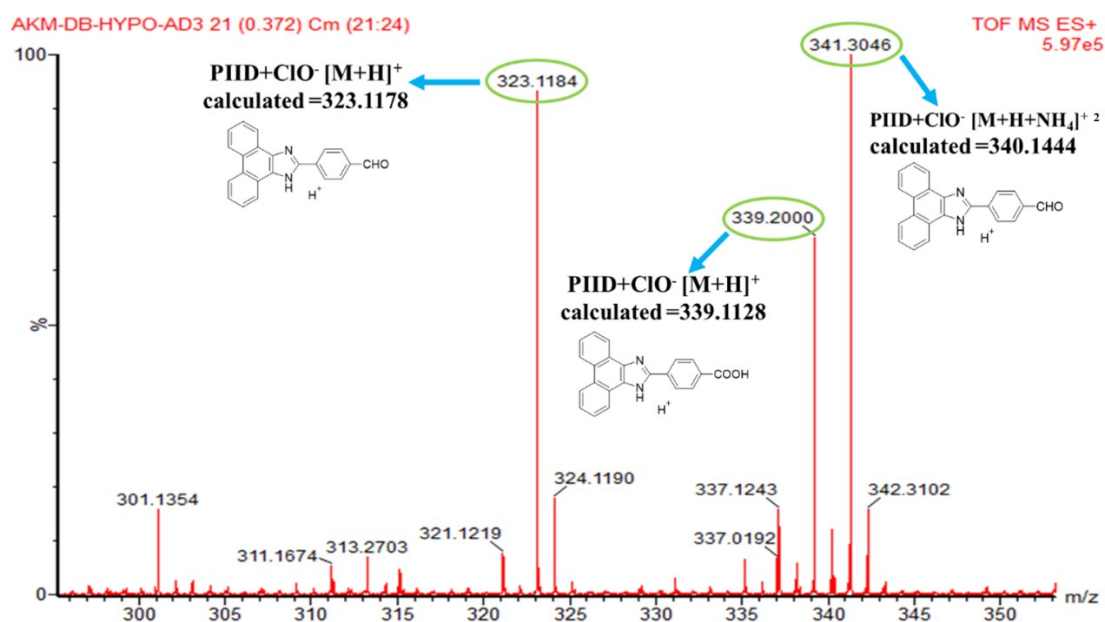


Fig. S12 HRMS spectra were taken from the reaction mixture of the probe **PIID** and excess of ClO^- .

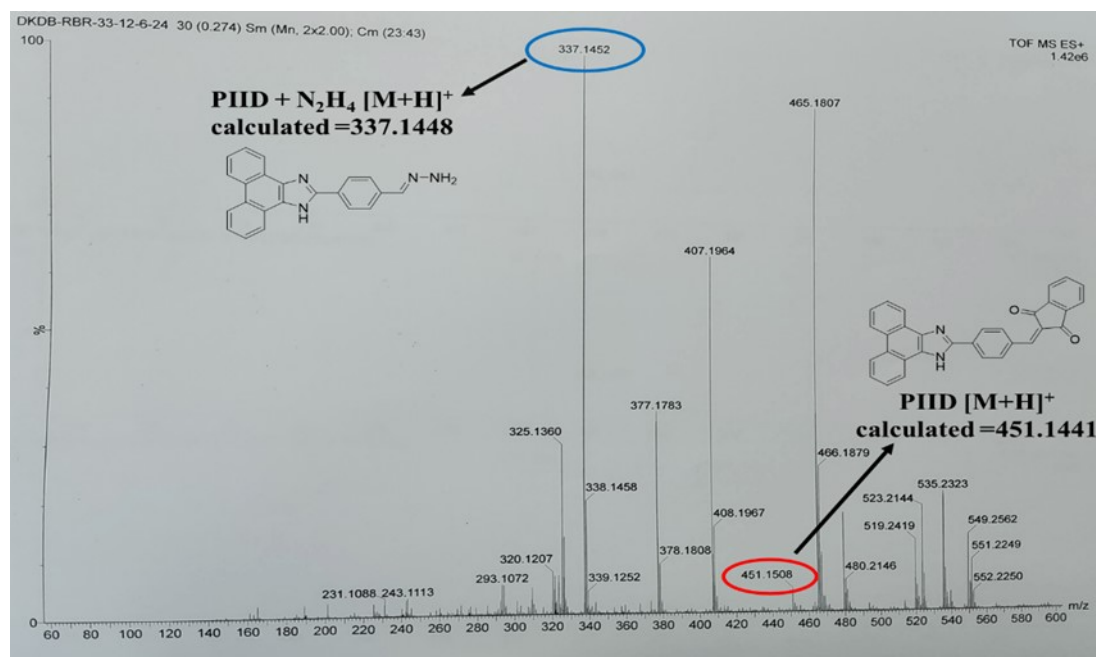


Fig. S13 HRMS spectra were taken from the reaction mixture of the probe **PIID** and excess hydrazine.

14. Table S2 The main vertical orbital transition of the Probe **PIID** and the resulting compounds **PIB** and **PIBH** calculated by TD-DFT method

Molecules	Energy (eV)	Wavelength (nm)	Osc. Strength (f)	Transition
PIID	2.3383	530.23	1.1313	HOMO → LUMO
	2.9579	419.17	0.0088	HOMO → LUMO+1
	2.9843	415.45	0.0134	HOMO-1 → LUMO
PIB	2.9206	424.51	0.8236	HOMO → LUMO
	3.4844	355.83	0.0123	HOMO-1 → LUMO
	3.6511	339.58	0.0001	HOMO-3 → LUMO
PIBH	3.2161	385.51	1.1030	HOMO → LUMO
	3.6363	340.96	0.0076	HOMO → LUMO+1
	3.8742	320.03	0.0296	HOMO → LUMO+2

15. MTT assay

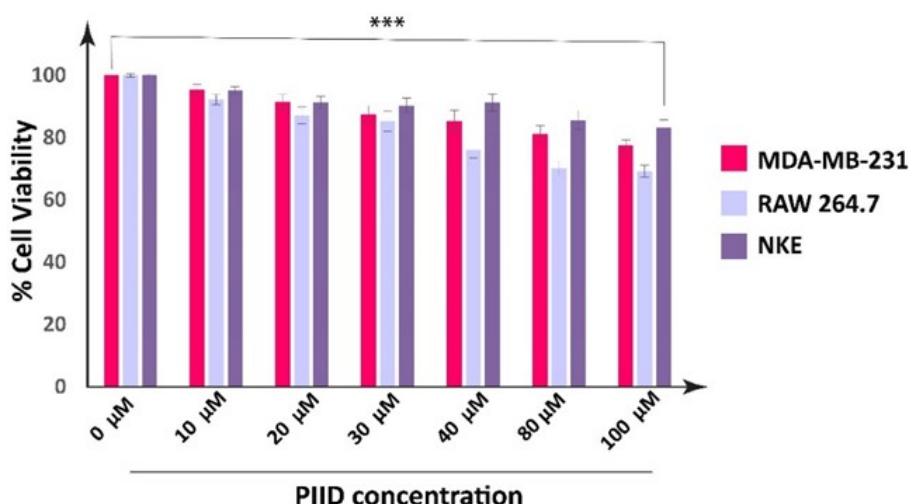


Fig. S14 Cell survivability of MDA-MB 231, RAW 264.7, and NKE cells exposed to different concentrations of probe **PIID**. Data represent at least three independent experiments, and the bar graph shows mean \pm SEM, *** $p < 0.0001$, were interpreted as statistically significant compared to the control.

16. Table S3 Environmental water sample study for ClO^- detection

Water sample	ClO^- spiked (μM)	Found (μM)	% Recovery	RSD (%)
Tap water	15	14.68 ± 0.25	97.86	1.70
	20	19.72 ± 0.22	98.60	1.12
Ganges River water	15	14.27 ± 0.27	95.13	1.89
	20	19.35 ± 0.25	96.75	1.29
Lake Water	15	14.45 ± 0.27	96.33	1.86
	20	19.56 ± 0.32	97.80	1.64

17. Table S4 Environmental water sample study for N_2H_4 detection

Water sample	N_2H_4 spiked (μM)	Found (μM)	% Recovery	RSD (%)
Tap water	30	29.65 ± 0.39	98.83	1.31
	40	39.72 ± 0.42	99.30	1.06
Ganges River water	30	28.51 ± 0.57	95.03	1.99
	40	39.18 ± 0.65	97.95	1.66
Lake Water	30	29.33 ± 0.36	97.76	1.23
	40	39.30 ± 0.45	98.25	1.14

18. Fluorescence spectra of the probe PIID for commercial sample

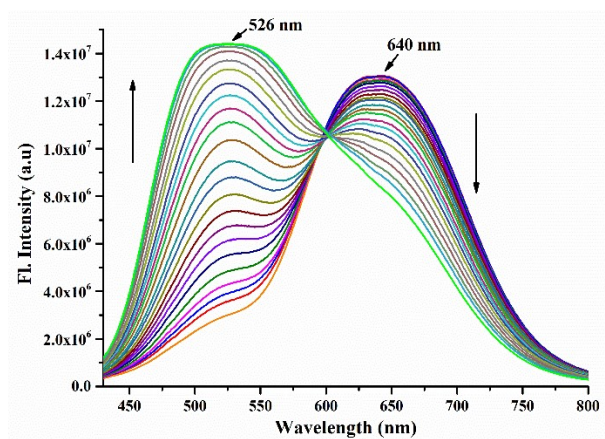


Fig. S15 Emission spectra of **PIID** (10 μM) upon the addition of increasing amounts of commercial disinfectant ($\lambda_{\text{ex}} = 420 \text{ nm}$).

19. NMR Spectra: ^1H -NMR, ^{13}C -NMR

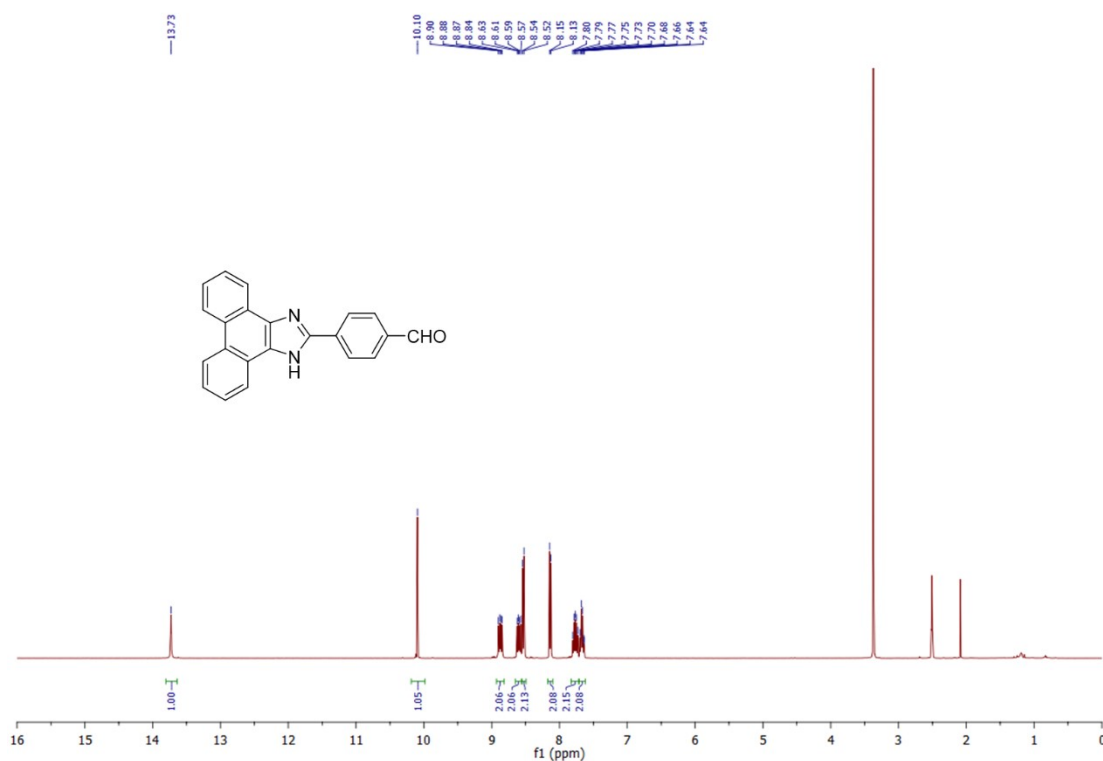


Fig. S16 ^1H NMR spectrum of the compound **PIB** in DMSO-d_6

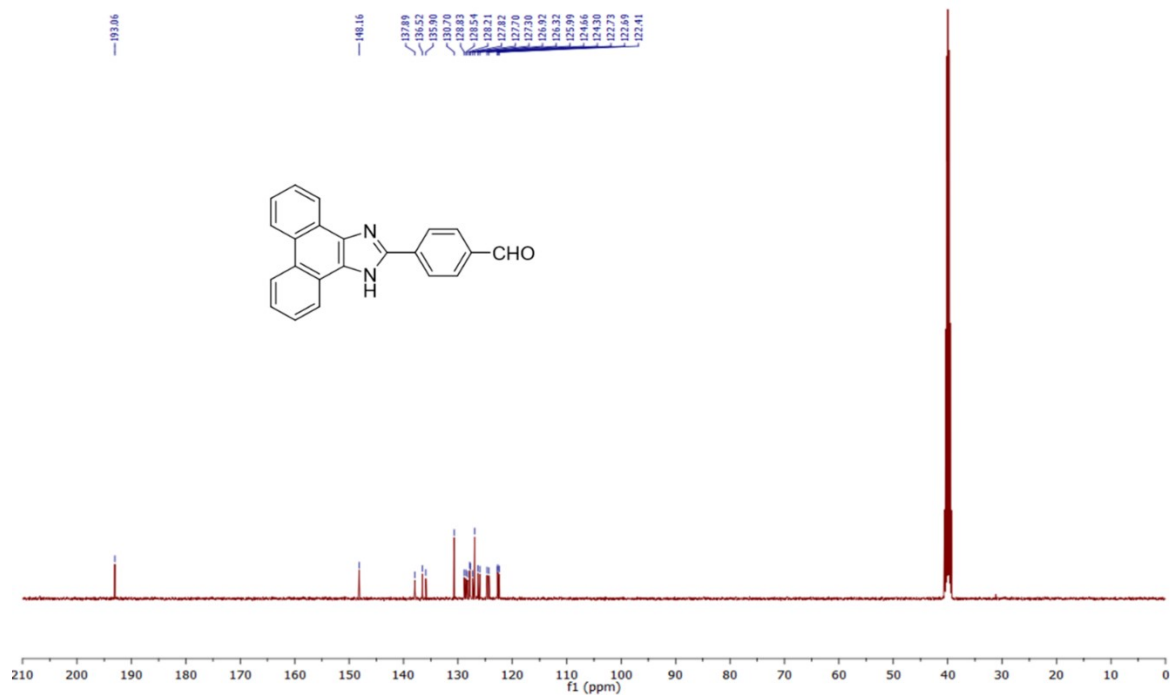


Fig. S17 ¹³C NMR spectrum of the compound **PIB** in DMSO-d₆

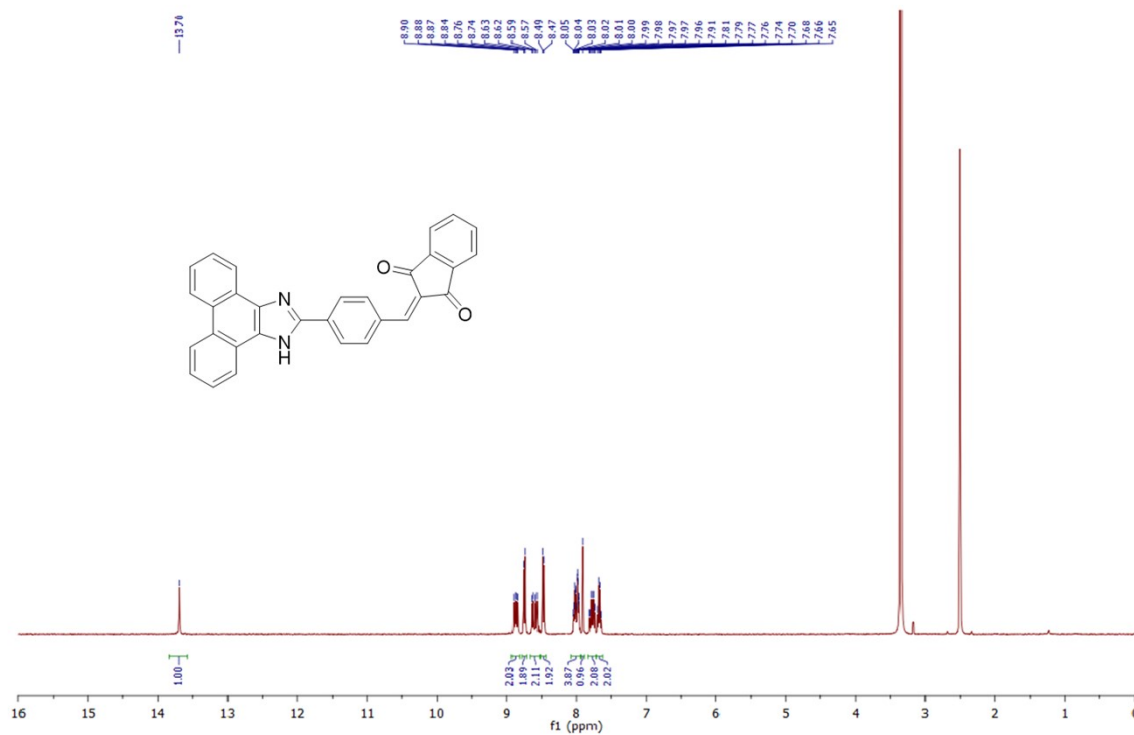


Fig. S18 ¹H NMR spectrum of the compound **PIID** in DMSO-d₆

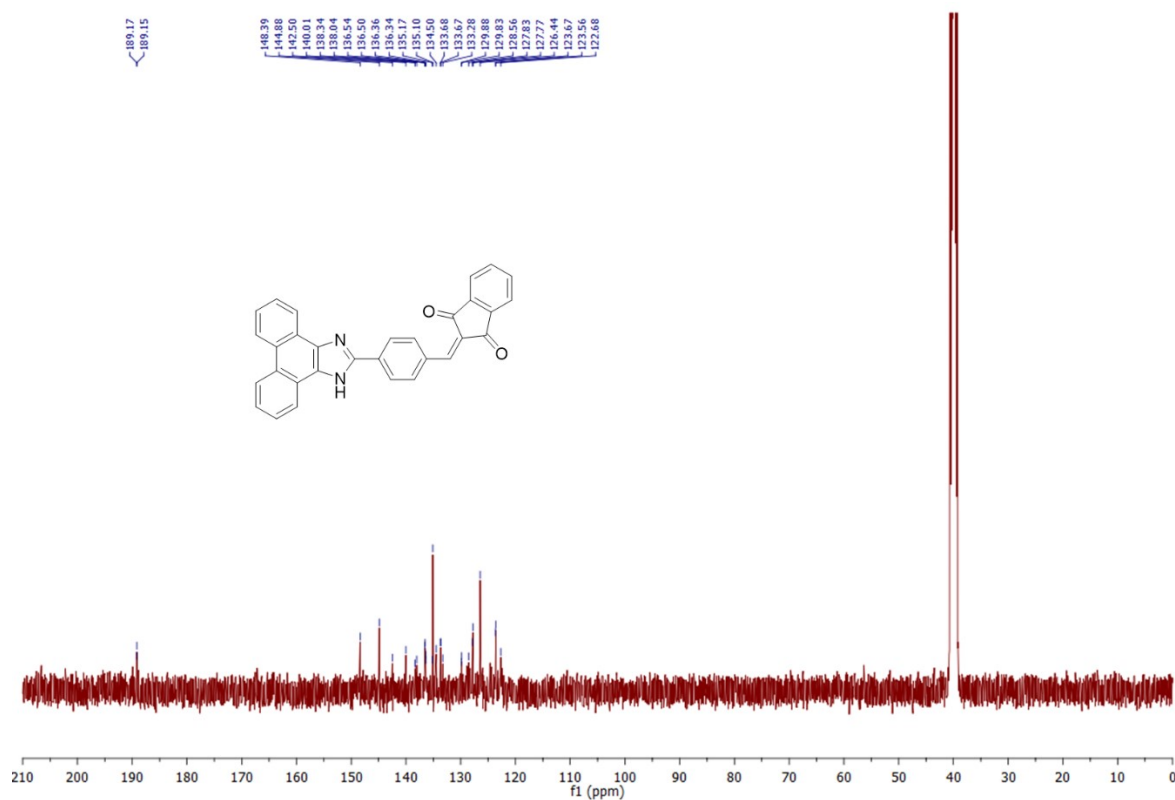


Fig. S19 ¹³C NMR spectrum of the compound PIID in DMSO-d₆

20. IR Spectra

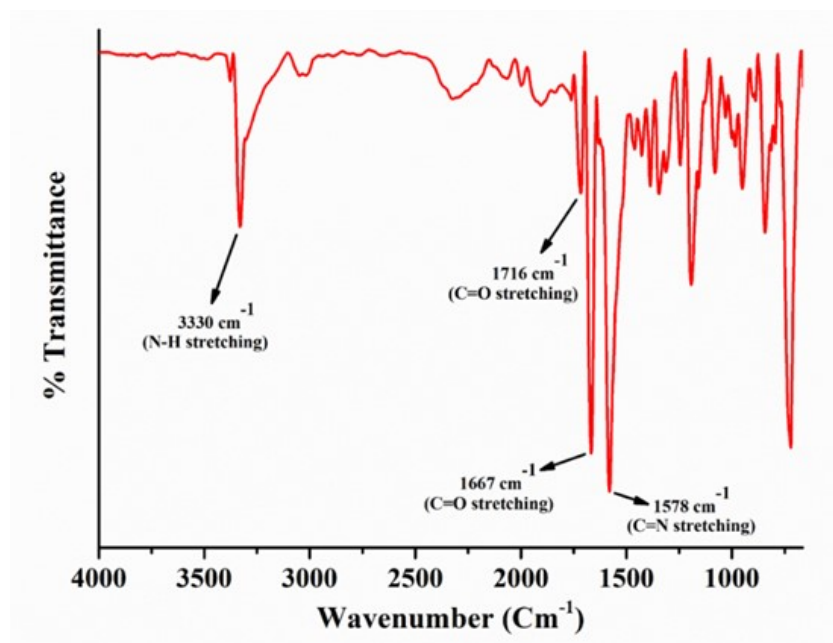


Fig. S20 The IR spectrum of the compound PIID

21. ESI-MS Spectra

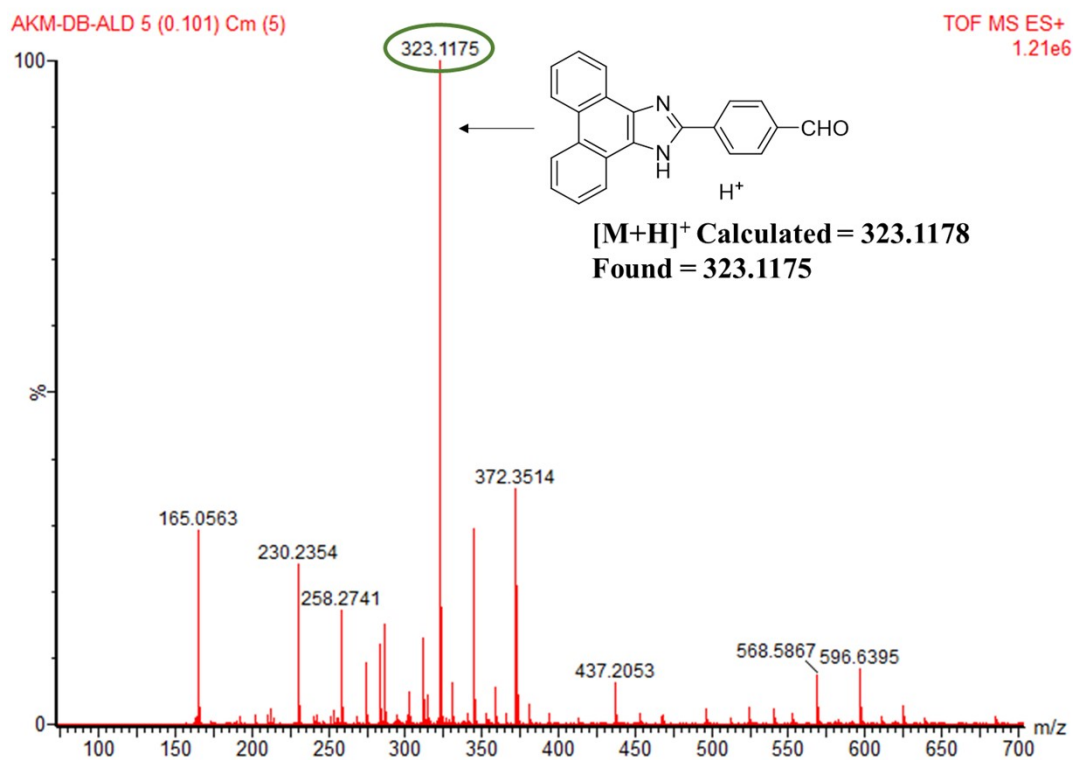


Fig. S21 HRMS spectra of the compound PIB

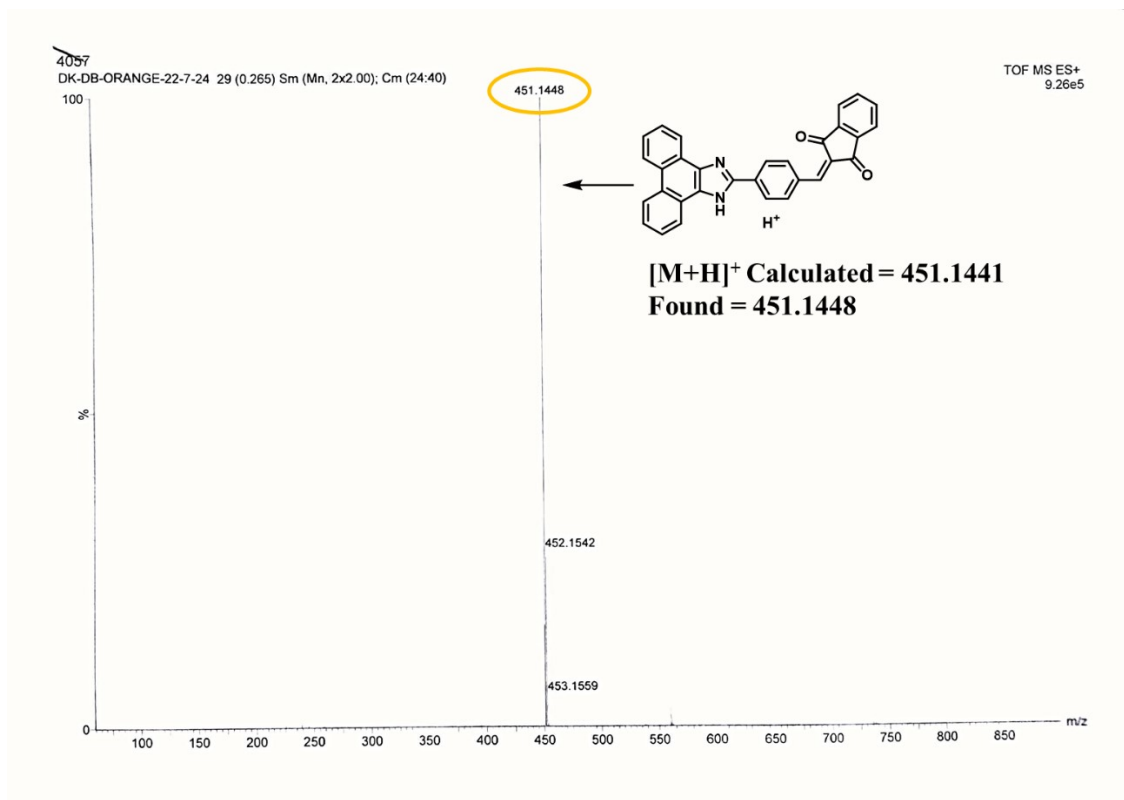
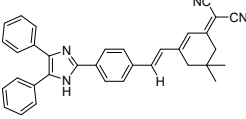
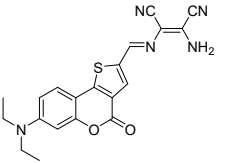
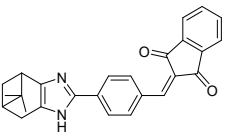
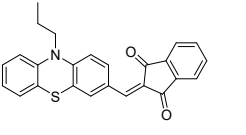
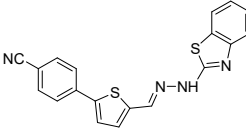
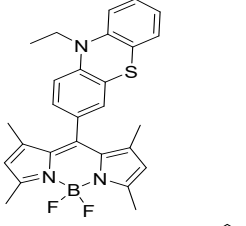
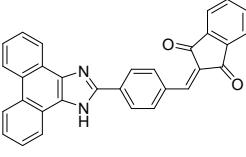
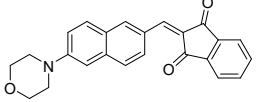
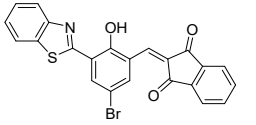
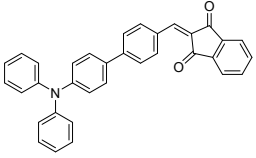
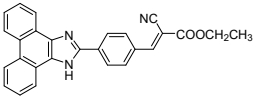
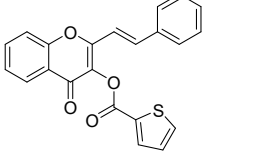
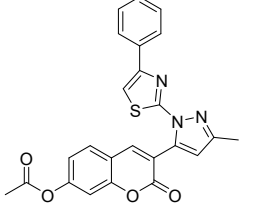
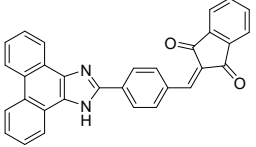


Fig. S22 HRMS spectra of the compound PIID

22. Table S5 Comparison table of important parameters between reported hypochlorite probes with our probe PIID

Structure of the probe	Solvent system	Mode of sensing	LOD	Stoke shift/Emission shift (nm)	Response time	Applications Water sample/Test strip/commercial sample	Exogenous/endogenous cell imaging	Cytotoxicity assay Human cancer cell line/human epithelial cell line	Ref
	DMSO: H ₂ O (6:4 v/v)	FL Turn-on, ICT	0.44 μ M	100/-	-	Yes/Yes/No	Yes/No	No/No	2
	PBS buffer (10 mM, pH = 7.4) containing CTAB (1.5 mM)	Ratiometric	94 nM	227/170	1 min	Yes/No/No	Yes/Yes	Yes/No	3
	THF/PBS buffer (v/v = 5/5, pH = 7.4)	Ratiometric, ICT	13.2 nM	241/140	0.5 min	Yes/Yes/No	Yes/Yes	Yes/No	4
	PBS aqueous buffer (DMSO: H ₂ O = 9:1, 20 mM, and pH = 7.4)	FL Turn-on/ ICT	24 nM	111/-	1 min	Yes/Yes/No	No/No	Yes/No	5
	DMSO/H ₂ O (4: 6, v/v)	Ratiometric, ICT	8.74 nM	116/93	80 sec	Yes/Yes/Yes	Yes/No	Yes/Yes	6
	PBS buffer (pH 7.4, 10 mM, containing 50% EtOH as a cosolvent)	FL Turn-on/ PET	1.7 nM	15/-	Few seconds	No/No/No	Yes/No	No/No	7
	THF/H ₂ O solution (3:7, v/v; 10 mM PBS buffer, pH 7.4)	Ratiometric, ICT	32.75 nM	220/114	40 sec	Yes/Yes/Yes	Yes/Yes	Yes/Yes	This work

23. Table S6 Comparison table of important parameters between reported hydrazine probes with our probe PIID

Structure of the probe	Solvent system	Mode of sensing	LOD	Stoke shift/Emission shift (nm)	Response time	Applications Water sample/Test strip/soil sample	Plant tissue imaging	Ref
	CH ₃ CN/PBS buffer (10.0 mM, pH = 7.4, 1/1, v/v)	Ratiometric, ICT	0.5 μ M	200/230	18 min	No/No/No	No	8
	DMSO/PBS buffer (v/v, 6/4, 10.0 mM, pH:7.4)	Ratiometric, ESIPT, ICT	1.29 μ M	80/170	2 min	Yes/Yes/Yes	Yes	9
	DMSO/H ₂ O v/v=8:2 and 1:9 pH=7.4	FL Turn-on or off/ AIE & ACQ	0.137 μ M	153/-	-	No/Yes/No	No	10
	DMSO/H ₂ O (6:4, v/v)	Ratiometric, ICT	1.6 μ M	205/87	15 min	No/No/No	No	11
	DMSO/ PBS buffer solution (v/v = 4/6,10 mmol·L ⁻¹ , pH = 7.4)	FL Turn-on/ ESIPT	0.14 μ M	100/-	25 min	Yes/Yes/No	No	12
	H ₂ O /DMF solution (v/v = 8/2)	FL Turn-on/ ICT	24 nM	74/-	30 min	Yes/No/No	No	13
	THF/H ₂ O solution (4:6, v/v; 10 mM PBS buffer, pH 7.4)	Ratiometric, ICT	92 nM	220/216	90 sec	Yes/Yes/Yes	Yes	This work

24. References

- (1) A. Dutta, S. Halder, I. Bhaumik, U. Debnath, D. Dhara, A. K. Misra, K. Jana, *ACS Pharmacol. Transl. Sci.*, 2024, **7**, 195–211.
- (2) Megha, P. Kaur, K. Singh, *Dyes Pigm.*, 2024, **228**, 112249.
- (3) L. Shi, H. Yu, X. Zeng, S. Yang, S. Gong, H. Xiang, K. Zhang, G. Shao, *New J. Chem.*, 2020, **44**, 6232.
- (4) Y. Zhang, H. Yang, M. Li, S. Gong, J. Song, Z. Wang, S. Wang, *Dyes Pigm.*, 2022, **197**, 109861.
- (5) H. Feng, Y. Wang, J. Liu, Z. Zhang, X. Yang, R. Chen, Q. Meng, R. Zhang, *J. Mater. Chem. B*, 2019, **7**, 3909.
- (6) S. Banerjee, D. Banik, S. Halder, A. Karak, P. Ghosh, K. Jana, A. K. Mahapatra, *Org. Biomol. Chem.*, 2024, **22**, 1662.
- (7) H. Lia, Y. Miaoa, Z. Liua, X. Wua, C. Piao, X. Zhou, *Dyes Pigm.*, 2020, **176**, 108192.
- (8) H. Su, J. Wang, X. Yue, B. Wang, X. Song, *Spectrochim Acta A Mol Biomol Spectrosc.*, 2022, **274**, 121096.
- (9) M. Oguza, S. Erdemira, S. Malkondu, *Anal. Chim. Acta*, 2022, **1227**, 340320.
- (10) D. Lia, L. Liua, H. Yanga, J. Maa, H. Wanga, J. Pan, *Materials Science & Engineering B*, 2022, **276**, 115556.
- (11) Z. Li, W. Zhang, C. Liu, M. Yu, H. Zhang, L. Guo, L. Wei, *Sens Actuators B Chem.*, 2017, **241**, 665-671.
- (12) A. Qin, Y. Zhang, S. Gong, M. Li, Y. Gao, X. Xu, J. Song, Z. Wang, S. Wang, *Front. Chem. Sci. Eng.*, 2023, **17**, 24–33.
- (13) X. Tian, M. Li, Y. Zhang, S. Gong, X. Wang, Z. Wang, S. Wang, *J. Photochem. Photobiol. A: Chem.*, 2023, **437**, 114467.